Supplement of

Exploring the ability of the variable-resolution CESM to simulate cryospheric-hydrological variables in High Mountain Asia

René R. Wijngaard[1,*], Adam R. Herrington[2], William H. Lipscomb[2], Gunter R. Leguy[2], and Soon-Il An[1,3]

[1]Irreversible Climate Change Research Center, Yonsei University, Seoul, South Korea
[2]Climate and Global Dynamics Laboratory, National Center for Atmospheric Research, Boulder CO, USA
[3]Climate Theory Lab, Department of Atmospheric Sciences, Yonsei University, Seoul, South Korea
[*]Now at: Institute for Marine and Atmospheric Research Utrecht, Utrecht University, Utrecht, the Netherlands

Correspondence to: Soon-Il An (sian@yonsei.ac.kr) and René R. Wijngaard (r.r.wijngaard.uu@gmail.com)

Section S1 CLM Glacier-Cover Dataset

For the HMA_VR7b simulation, we updated the CLM glacier-cover dataset to represent glacier and ice sheet cover more accurately. In the original dataset, we found large deviations in parts of HMA between the mean CLM grid cell elevation and the mean glacier elevation derived from the glacier-cover dataset (Figure S1a). These deviations, which were largest in southeastern HMA, are mainly attributable to inaccuracies of the Randolph Glacier Inventory (RGI) version 1 (RGI-Consortium, 2012) glacier outlines used to create the original dataset (Figure S1b).

The updated glacier-cover dataset encompasses three 3-minute datasets: 1) fractional land ice coverage, including both glaciers and ice sheets, 2) distributions of areal glacier coverage by elevation, and 3) distributions of areal ice-sheet coverage by elevation. Figure S2 summarizes the workflow to generate the updated dataset. The fractional land ice coverage and distributions by elevation are derived from global glacier outlines, vector data of ice-sheet coverage, and a global 30-arcsec elevation dataset and land-sea mask. The global glacier outlines are retrieved from the Randolph Glacier Inventory version 6 (RGI-Consortium, 2017), and the vector data for the Greenland and Antarctic ice sheets are retrieved from the masks of BedMachine version 4 (Morlighem et al., 2017, 2021) and version 2 (Morlighem et al., 2020; Morlighem, 2020), respectively. The global elevation data and land-sea mask are obtained from a merged BedMachine/GMTED2010 product in which the higher-resolution BedMachine datasets are conservatively regridded to the 30-arcsec GMTED2010 grid, overwriting the GMTED2010 Greenland and Antarctica values. First, 30-arcsec polygon grids are generated, which are overlaid with global glacier outlines and ice-sheet vector data, respectively, to calculate ice percent cover in each polygon grid cell. The polygon grid cells are then concatenated, followed by the rasterization of the polygon grids. This results in two 30-arcsec land ice masks containing fractional ice coverage for glaciers and ice sheets, respectively. Second, the land ice masks are draped over global

30-arcsec elevation data. In each grid cell, ice fractions are distributed over 70 elevation bins (at 100 m intervals) and an additional bin that includes ice cover above 7000 m, resulting in 30-arcsec distributions of areal ice coverage by elevation for glaciers and ice sheets. Third, the elevation distributions are conservatively regridded to 3-minute resolution and aggregated to generate 3-minute distributions of fractional land ice coverage. Finally, the land-sea mask is conservatively regridded to 3-minute resolution and is corrected by defining grid cells as land where ice cover (including floating ice shelves) is present.

Given the new CLM surface datasets, the distributions by elevation are used to subdivide each CLM glacier land unit into columns based on the 36 ECs defined above. More detailed information about the original glacier-cover dataset can be found in the CLM5 Documentation (https://escomp.github.io/ctsm-docs/). Differences between the original and updated datasets are listed in Table S1.

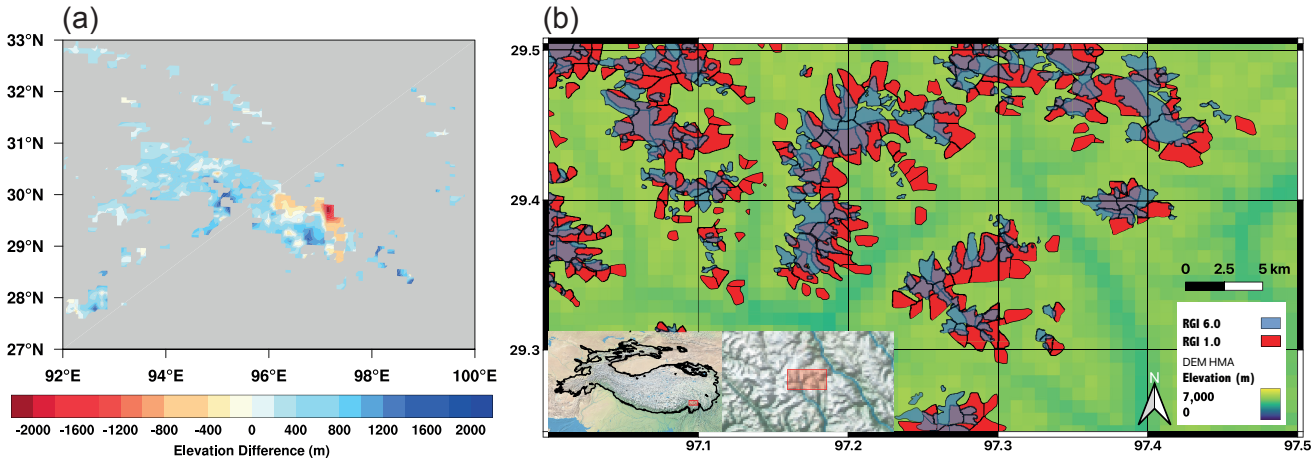

Figure S1. (**a**) Differences between the mean elevation of the CLM grid cell and the mean glacier elevation within the grid cell. (**b**) Glacier outlines retrieved from Randolph Glacier Inventory version 1 (red) and version 6 (blue) (RGI-Consortium, 2012, 2017). The background elevation data is retrieved from Natural Earth. The red box in the insets denote the location of the glacier outlines and the black outline represents the outline of High Mountain Asia, where the HMA outlines are retrieved from the Global Mountain Biodiversity Assessment (GMBA) Mountain Inventory version 1.2 (Körner et al., 2017). The location of the red box is based on the large negative elevation differences in Figure S1a.

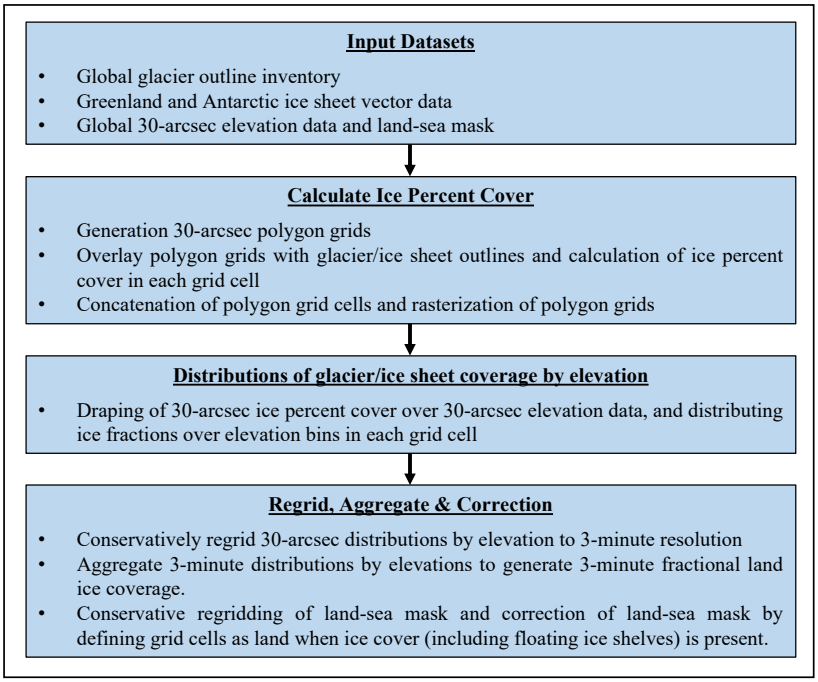

Figure S2. Schematic overview of workflow used for generating the updated CLM glacier-cover dataset.

Table S1. Overview of the input datasets that have been used for the original (v1) and updated (v2) CLM glacier-cover datasets, and the differences in the number of elevation bins that are used among the different glacier-cover datasets.

	CLM glacier-cover dataset v1	**CLM glacier-cover dataset v2**
Glacier outlines	Randolph Glacier Inventory v1 (RGI-Consortium, 2012)	Randolph Glacier Inventory v6 (RGI-Consortium, 2017)
Greenland ice sheet outlines	University of Zurich Raster Data (Rastner et al., 2012)	BedMachine v4 (Morlighem et al., 2017, 2021)
Antarctica ice sheet outlines	SCAR Antarctic Digital Database v5 (ADD Consortium, 2000; Fox et al., 1994)	BedMachine v2 (Morlighem et al., 2020; Morlighem, 2020)
Topography	GLOBE Topography (Hastings et al., 1999)	GMTED2010 (glaciers) + BedMachine (icesheets) (Morlighem et al., 2017, 2020; Danielson and Gesch, 2011)
No. of elevation bins (100 m interval)	60 (< 6000 m) + 1 (6000 – 10,000 m)	70 (< 7000 m) + 1 (7000 – 10,000 m)

Section S2 Supplementary Figures and Tables

Table S2. Mean winter (DJF) and summer (JJA) 2m temperature, rainfall, snowfall, snow cover, and snow depth for NE30, HMA_VR7a, HMA_VR7b, WFDEI (temperature + precipitation), NSIDC (snow cover), and HARv2 (snow depth). The seasonal means/sums are calculated over the HMA subregions (Figure 1b) for the period 1979–1998 (1980 –1998 for HARv2).

	SW-HMA		**SE-HMA**		**NW-HMA**		**NE-HMA**	
2m Temperature (°C)	**DJF**	**JJA**	**DJF**	**JJA**	**DJF**	**JJA**	**DJF**	**JJA**
NE30	-12	13	-1	15	-9	18	-14	12
HMA_VR7a	-16	10	-2	14	-11	16	-14	12
HMA_VR7b	-15	10	-1	14	-11	17	-14	12
WFDEI	-8	12	0	15	-10	16	-12	10
Rainfall (mm)	**DJF**	**JJA**	**DJF**	**JJA**	**DJF**	**JJA**	**DJF**	**JJA**
NE30	25	383	52	1109	14	84	1	342
HMA_VR7a	21	420	37	1171	11	82	0.4	290
HMA_VR7b	19	435	37	1130	11	84	0.3	281
WFDEI	48	145	38	740	16	75	1	163
Snowfall (mm)	**DJF**	**JJA**	**DJF**	**JJA**	**DJF**	**JJA**	**DJF**	**JJA**
NE30	237	9	76	4	62	2	30	20
HMA_VR7a	193	33	58	41	50	12	17	34
HMA_VR7b	208	43	62	53	61	14	19	39
WFDEI	99	12	23	50	45	3	9	18
Snow Cover (%)	**DJF**	**JJA**	**DJF**	**JJA**	**DJF**	**JJA**	**DJF**	**JJA**
NE30	81	2	30	0.1	66	0.2	61	0.2
HMA_VR7a	83	5	28	2	65	1	53	1
HMA_VR7b	83	7	28	2	67	1	52	1
NSIDC	75	42	24	9	68	17	25	2
Snow Depth (mm w.e.)	**DJF**	**JJA**	**DJF**	**JJA**	**DJF**	**JJA**	**DJF**	**JJA**
NE30	157	27	26	0.6	42	2	22	0.2
HMA_VR7a	121	24	27	8	38	1	15	0.4
HMA_VR7b	130	39	50	28	43	2	16	1
HARv2	96	34	17	5	57	4	14	1

Table S3. Mean integrated SMB mass fluxes (Gt yr^{-1}) for the period 1979–1998 (1979–1981 for HMALO simulations) in gigatons per year. The numbers in brackets denote the standard deviation in time. The integrated SMB mass fluxes have been calculated over two different areas of integration for HMA_VR7a, derived from the original and updated glacier-cover datasets, respectively. The SMB mass fluxes for HMA_VR7a (HMALOa) that are integrated over the glacier areas of the updated glacier-cover dataset are denoted as HMA_VR7a_GC2 (HMALOa_GC2). The mass fluxes of HMA_VR7b (HMALOb) are only integrated over the glacier areas of the updated dataset.

Simulation	Glacier	Precipitation	Ice Melt	Total	Refreezing	Runoff	Sublimation/	SMB
HMA_VR7a	120,087	111 (6)	463 (33)	553 (29)	34 (2)	554 (33)	15 (1)	-459
HMA_VR7a_GC2	96,493	90 (5)	356 (26)	432 (23)	29 (2)	430 (26)	12 (0.6)	-352
HMA_VR7b	96,493	93 (4)	228 (20)	324 (18)	32 (2)	306 (21)	12 (0.5)	-224
HMALOa_GC2	96,493	47 (2)	463 (14)	501 (9)	13 (2)	492 (12)	19 (1.0)	-464
HMALOb	96,493	46 (2)	333 (19)	385 (8)	16 (5)	367 (12)	19 (0.9)	-339

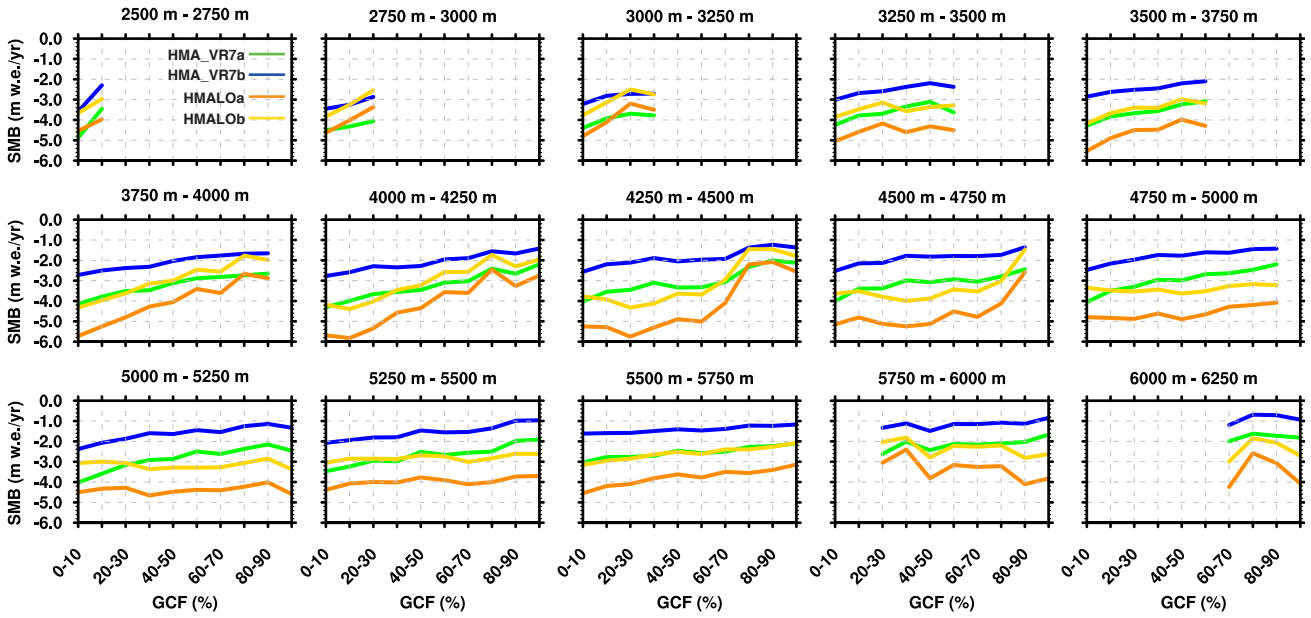

Figure S3. CLM grid-cell-mean SMB-glacier fraction distributions for HMALOa (orange), HMALOb (yellow) HMA_VR7a (green), and HMA_VR7b (blue). The SMB–glacier elevation distributions are calculated for 15 different 250m elevation zones between 2500 m and 6250 m altitude, where elevation zones are based on CLM grid-cell-mean elevation distributions.

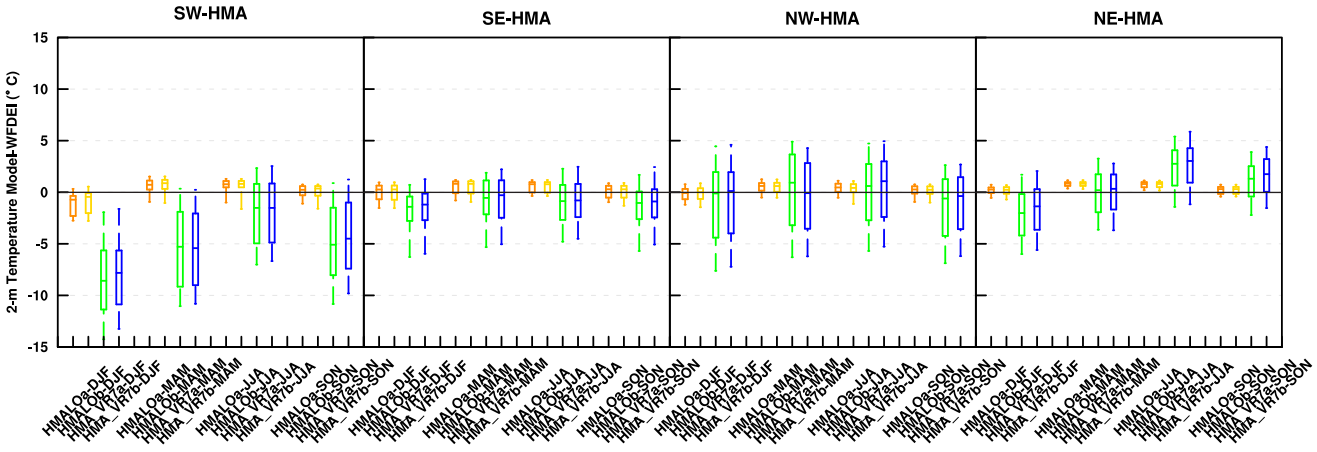

Figure S4. Boxplots of 2-m temperature differences (°C) between the simulation outputs of HMALOa (orange), HMALOb (yellow), HMA_VR7a (green), HMA_VR7b (blue), and the observation/reanalysis-based WFDEI for each season and HMA subregion (shown in Figure 1b). The box represents the biases between the 25th and 75th percentile, the line in the box denotes the median, and the whiskers represent the 10th and 90th percentile of temperature differences.

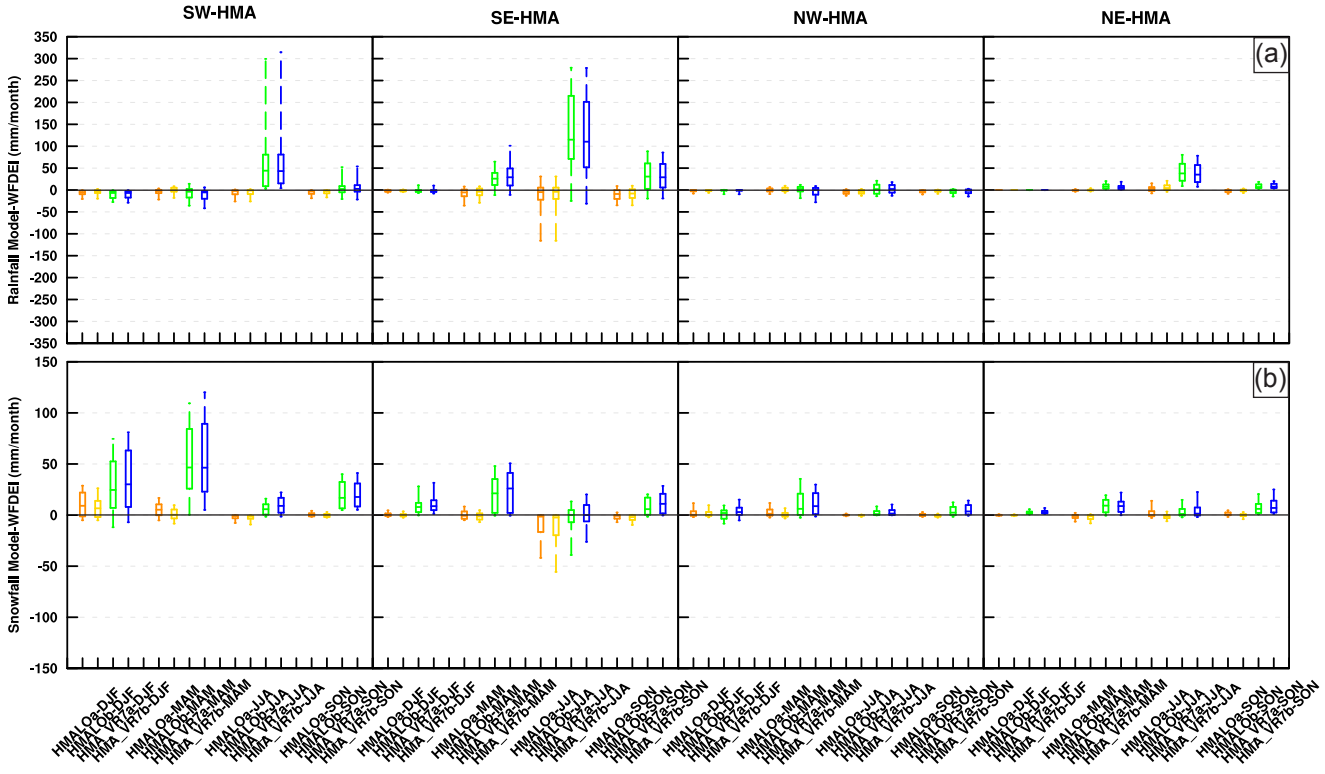

Figure S5. Same as Figure RC1.1, but for rainfall (mm month^{-1}) (**a**) and snowfall (mm month^{-1}) (**b**)

References

ADD Consortium: Antarctic Digital Database, Version 3.0, database, manual and bibliography, Cambridge, 2000.

Danielson, J. J. and Gesch, D. B.: Global Multi-resolution Terrain Elevation Data 2010 (GMTED2010), U.S. Geological Survey Open-File Report 2011-1073, 2011.

Fox, A. J., Paul, A., and Cooper, R.: Measured Properties of the Antarctic Ice Sheet Derived from the Scar Antarctic Digital Database, Polar Record, 30, https://doi.org/10.1017/S0032247400024268, 1994.

Hastings, D. A., Dunbar, P. K., Elphingstone, G. M., Bootz, M., Murakami, H., Maruyama, H., Masaharu, H., Holland, P., Payne, J., Bryant, N. A., Logan, T. L., Muller, J.-P., Schreier, G., and MacDonald, J. S.: The Global Land One-kilometer Base Elevation (GLOBE) Digital Elevation Model, Version 1.0, Boulder, Colorado, USA, 1999.

Körner, C., Jetz, W., Paulsen, J., Payne, D., Rudmann-Maurer, K., and M. Spehn, E.: A global inventory of mountains for bio-geographical applications, Alp Bot, 127, https://doi.org/10.1007/s00035-016-0182-6, 2017.

Morlighem, M.: MEaSUREs BedMachine Antarctica, Version 2 , Boulder, Colorado USA. NASA National Snow and Ice Data Center Distributed Active Archive Center, https://doi.org/10.5067/E1QL9HFQ7A8M, 2020.

Morlighem, M., Williams, C. N., Rignot, E., An, L., Arndt, J. E., Bamber, J. L., Catania, G., Chauché, N., Dowdeswell, J. A., Dorschel, B., Fenty, I., Hogan, K., Howat, I., Hubbard, A., Jakobsson, M., Jordan, T. M., Kjeldsen, K. K., Millan, R., Mayer, L., Mouginot, J., Noël, B. P. Y., O'Cofaigh, C., Palmer, S., Rysgaard, S., Seroussi, H., Siegert, M. J., Slabon, P., Straneo, F., van den Broeke, M. R., Weinrebe, W., Wood, M., and Zinglersen, K. B.: BedMachine v3: Complete Bed Topography and Ocean Bathymetry Mapping of Greenland From Multibeam Echo Sounding Combined With Mass Conservation, Geophys Res Lett, 44, https://doi.org/10.1002/2017GL074954, 2017.

Morlighem, M., Rignot, E., Binder, T., Blankenship, D., Drews, R., Eagles, G., Eisen, O., Ferraccioli, F., Forsberg, R., Fretwell, P., Goel, V., Greenbaum, J. S., Gudmundsson, H., Guo, J., Helm, V., Hofstede, C., Howat, I., Humbert, A., Jokat, W., Karlsson, N. B., Lee, W. S., Matsuoka, K., Millan, R., Mouginot, J., Paden, J., Pattyn, F., Roberts, J., Rosier, S., Ruppel, A., Seroussi, H., Smith, E. C., Steinhage, D., Sun, B., Broeke, M. R. van den, Ommen, T. D. van, Wessem, M. van, and Young, D. A.: Deep glacial troughs and stabilizing ridges unveiled beneath the margins of the Antarctic ice sheet, Nat Geosci, 13, https://doi.org/10.1038/s41561-019-0510-8, 2020.

Morlighem, M., Williams, C. N., Rignot, E., An, L., Arndt, J. E., Bamber, J. L., Catania, G., Chauché, N., Dowdeswell, J. A., Dorschel, B., Fenty, I., Hogan, K., Howat, I., Hubbard, A., Jakobsson, M., Jordan, T. M., Kjeldsen, K. K., Millan, R., Mayer, L., Mouginot, J., Noël, B. P. Y., O'Cofaigh, C., Palmer, S., Rysgaard, S., Seroussi, H., Siegert, M. J., Slabon, P., Straneo, F., van den Broeke, M. R., Weinrebe, W., Wood, M., and Zinglersen, K. B.: IceBridge BedMachine Greenland, Version 4, Boulder, Colorado USA. NASA National Snow and Ice Data Center Distributed Active Archive Center, https://doi.org/10.5067/VLJ5YXKCNGXO, 2021.

Rastner, P., Bolch, T., Mölg, N., MacHguth, H., le Bris, R., and Paul, F.: The first complete inventory of the local glaciers and ice caps on Greenland, Cryosphere, 6, https://doi.org/10.5194/tc-6-1483-2012, 2012.
RGI-Consortium: Randolph Glacier Inventory - A Dataset of Global Glacier Outlines: Version 1.0, Boulder, Colorado, USA, https://doi.org/10.7265/p9yk-6m11, 2012.

RGI-Consortium: Randolph Glacier Inventory–A Dataset of Global Glacier Outlines: Version 6.0, Technical Report, Global Land Ice Measurements from Space, Colorado, USA, Boulder, Colorado, USA, https://doi.org/10.7265/4m1f-gd79, 2017.